

Cluster formation through the action of a single picosecond laser pulse

N. R. Madsen*, E. G. Gamaly, A. V. Rode and B. Luther-Davies

Laser Physics Centre, Research School of Physical Sciences and Engineering
The Australian National University, Canberra, ACT 0200, Australia

*nathan.madsen@anu.edu.au

Abstract. We demonstrate experimentally and describe theoretically the formation of carbon nanoclusters created by single picosecond laser pulses. We show that the average size of a nanocluster is determined exclusively by single laser pulse parameters and is independent of the gas fill (He, Ar, Kr, Xe) and pressure in a range from 20mTorr to 200 Torr. Simple kinetic theory allows estimates to be made of the cluster size, which are in qualitative agreement with the experimental data. We conclude that the role of the buffer gas is to induce a transition between thin solid film formation on the substrate and foam formation by diffusing the clusters through the gas, with no significant effect upon the average cluster size.

1. Introduction

Laser ablation has proven to be an efficient method for producing nanoclusters of different atomic content, shape and internal structure. Moreover, the size of a cluster has a significant effect upon various material properties and, therefore, provides a relatively simple experimental avenue to control those properties [1]. In this work we are, therefore, attempting to control the properties of carbon nanofoam via control over the size of carbon nanoclusters which are the “building blocks” for this material. To create the nanofoam we have used the standard approach where a laser ablates a target into an ambient gas. The gas serves to confine the ablated atomic plume reducing its diffusion velocity and therefore retaining the atoms at a temperature and density high enough for efficient atom-to-atom sticky collisions that result in cluster formation.

We report here experiments producing carbon nanoclusters that investigate the influence of scanning speed, gas fill type and pressure (including vacuum conditions), and laser fluence. We demonstrate that the adiabatic expansion time after the end of a single pulse, when the temperature and density of carbons are appropriate for cluster formation through atom-to-atom and atom-to-cluster attachment, appears to be sufficient for the many collisions to occur and this dominates nanocluster formation. In fact the plume expansion time for cluster formation in vacuum, which depends on the laser parameters, is the only significant factor determining the cluster size. This time it is similar to diffusion time in an ambient gas environment.

In what follows we describe the experimental set-up, diagnostics, and results for cluster distribution by sizes in the different experimental conditions. We then present simple estimates of the average cluster size and compare them to our experimental data and to recently published results of silicon cluster formation [2].

2. Experimental set-up and diagnostics

Carbon nanofoams were made using high power frequency doubled Nd:YVO₄ laser [3] operating at second harmonic (532 nm), with repetition rate 1.5 MHz, pulse duration 12 ps and focal spot size as small \approx 15 microns. This gave a maximum incident intensity of 7×10^{11} W/cm² with corresponding fluence 8.6 J/cm². The intensity and fluence could be varied to below the ablation threshold by increasing the spot size. The threshold fluence, defined as the fluence required to remove a single atomic layer from the target surface in a single pulse, was found to be 0.07 J/cm² for glassy carbon and 0.23 J/cm² for graphite using argon as the background gas at atmospheric pressure. To avoid drilling of the target surface the laser was scanned using x-y scanning mirrors in a constant velocity (maximum velocity of 1ms⁻¹) spiral pattern of overall diameter 5mm.

The results presented here were obtained from transmission electron microscope (TEM) images taken of carbon nanofoam created in different laser and chamber parameters and these were used to determine the average cluster sizes from the different nanofoam samples. The foam was deposited upon copper TEM grids which had been coated with holey carbon films (hole size 10-1000s of nm). A two second ablation exposure onto a grid approximately 1cm from the target ensured individual clusters could be seen as-deposited in a web-like arrangement, which arises due to the propagation of foam through the background gas. Cluster size distributions were generated with 10 calibrated images and most cases, about 500 clusters were used to generate a cluster size distribution which was then fitted with a best-fit Poissonian distribution to obtain an indication of the average size.

3. Experimental Results

A series of experiments were conducted to investigate the dependence of the cluster size upon various experimental parameters. These parameters included the laser scanning speed, background argon pressure and the type of filling gas. In the experiments presented in figure 1 both graphite and glassy carbon targets are used.

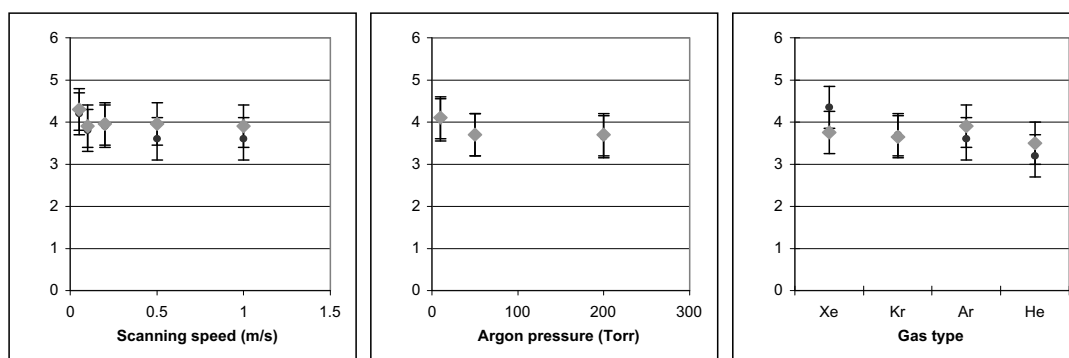


Figure 1. Measured cluster size for different experimental parameters. Glassy carbon target data is black circles while graphite target is the grey diamonds. Some data points overlap.

It is clear from the data that there is little if any significant difference in measured average cluster size for the parameters shown. The sets of experimental results regarding argon pressure and background filling gas type are important in that the lack of variance in cluster size indicates that there is little or no effect of the buffer gas upon the density of carbon in the cluster forming region. Combining this result with the result for cluster size at different scanning speed suggests that clusters form from the action of single pulses regardless of the presence of a buffer gas. As a result, it is necessary to investigate the appearance of deposited material at different pressures since these observations imply that clusters should be found deposited upon substrates even in vacuum conditions.

Figure 2 contains TEM images depicting the transitional nature of material deposition as the pressure is increased from effectively vacuum, where mean free path is greater than the distance to the substrate, to 2 Torr. Clearly for the vacuum situation (pressure 20mTorr) in the left image, the holey

carbon grid is coated with a thin solid layer, however, closer inspection reveals that the film is composed of aggregated clusters similar in size to those observed in the presence of a background gas. These clusters were visible around the edges of the film where the contrast is great enough for them to stand out. In the middle image, the pressure has been increased to 200mTorr and it is clear now that the presence of a buffer gas is beginning to introduce a more foam-like appearance to the deposited material due the presence of collisions as the plume propagates to the substrate. Finally, the image on the right shows material produced at 2 Torr displaying the expected structure achieved through deposition of clusters in the presence of a background gas.

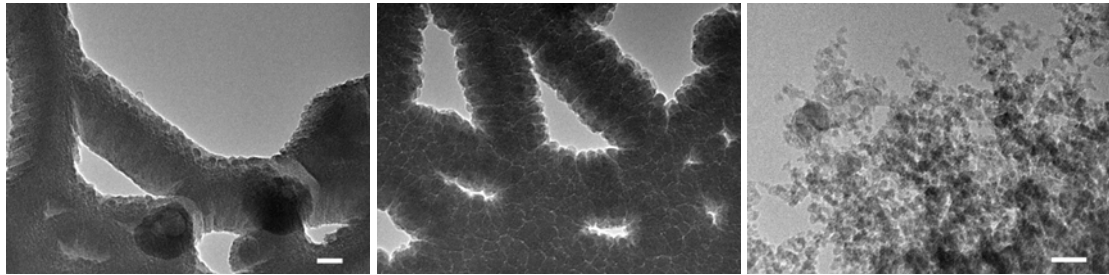


Figure 2. TEM images of carbon nanocluster material created at various pressures. From left to right the images depict material created at 20 mTorr, 200mTorr and 2 Torr respectively. The scale bar in the left image also corresponds to the middle image. Both scale bars are 25 nm.

To say with certainty that the clusters seen in vacuum are the same as those seen in the presence of a buffer gas requires cluster size distributions to be created for both cases. Hence clusters need to be found in vacuum deposited individually upon substrates. Such clusters could be found on grids in shadowed areas where diamond-like carbon material was not deposited. The low magnification image on the left of figure 3 shows a region, in the centre of the image, shadowed from the ablation source by the edge of a copper TEM grid where clusters were individually deposited on the holey carbon film.

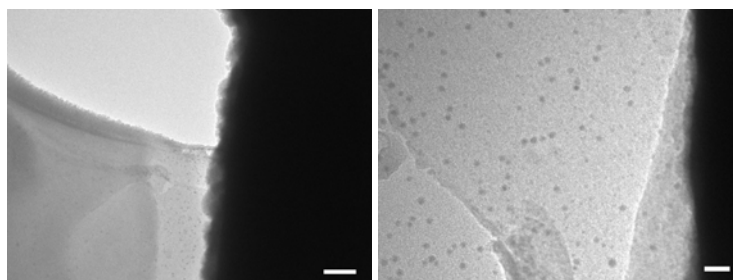
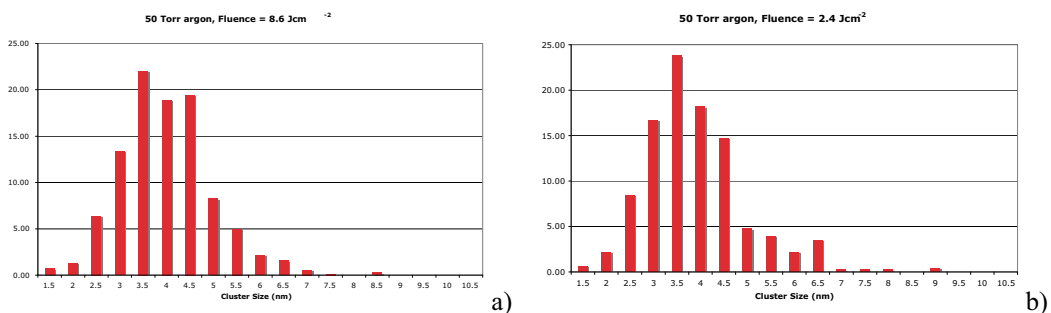


Figure 3. TEM images of deposited material in vacuum (20mTorr). Left image is low magnification with the scale bar representing 100nm while the scale bar on the left is 25nm.



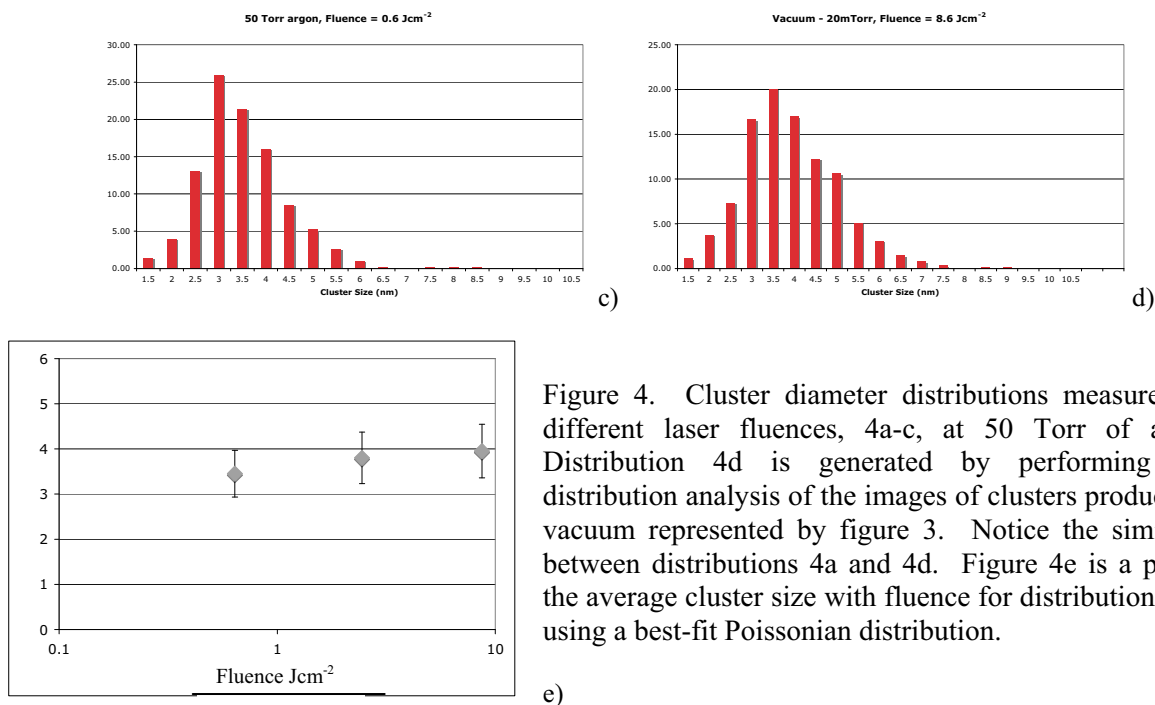


Figure 4. Cluster diameter distributions measured for different laser fluences, 4a-c, at 50 Torr of argon. Distribution 4d is generated by performing size distribution analysis of the images of clusters produced in vacuum represented by figure 3. Notice the similarity between distributions 4a and 4d. Figure 4e is a plot of the average cluster size with fluence for distributions 4a-c using a best-fit Poissonian distribution.

In addition to generating a cluster size distribution for individual clusters seen in the above images, experiments were conducted to investigate the dependence of cluster size upon laser fluence. Our experiments imply that in the parameters of these experiments, clusters form from a single laser pulse, hence the laser parameters should effect the cluster size. Nanofoam was therefore produced in an argon atmosphere of 50 Torr at fluences of 8.6, 2.4 and 0.6 J/cm². Figure 4 contains cluster size distributions measured for the three different fluences in addition to a cluster size distribution generated from images of individual clusters found in shaded areas of vacuum deposited samples. It is clear, as shown in figure 4e that as the fluence is decreased there is a corresponding weak decrease in the measured average cluster size. Also it is important to note the similarity of figures 4a (average = 3.9nm) and 4d (average = 3.95nm) indicating that clusters formed at 50 Torr are the same size as those produced in vacuum conditions.

In the next section theoretical considerations will be made to obtain simple estimates of the average cluster size in vacuum and in a buffer gas.

4. Estimates for the maximum size of clusters formed near the ablating target

In what follows we present a simple model of cluster formation by a single pulse and estimate the cluster size as a function of laser parameters. The cluster formation scenario is as follows. First, the flow of hot carbons is created during ablation. The laser pulse duration is too short for the clusters to be formed during the pulse. Therefore, after the end of the pulse the ablated vapours either diffuse, when the chamber is filled with a gas, or vapours adiabatically expand into vacuum. The cluster formation process is considered as a consequence of atom-to-atom and atom-to-cluster sticky collisions under the assumption that the monomer addition process dominates nucleation.

4.1. Flow of ablated carbons after the end of the laser pulse

The maximum kinetic energy per ablated ion is defined as follows [4,5]:

$$T_{m,kin} = T_o = \frac{4(F_a - F_{thr})}{3 \cdot n_a \cdot l_{abs}} \quad (1)$$

Here F_a is the absorbed laser fluence, l_{abs} is the absorption depth, and n_a is the atomic number density of the target. Above we accounted for the losses on ablation and ionization. The ablation threshold reads [5]:

$$F_{th} \approx \frac{3}{4} \frac{n l_{abs} (\varepsilon_b + J)}{A} \quad (2)$$

where ε_b is the binding energy and J is the first ionisation potential. We express the ablated depth in a simplified form as the average between two limit cases, $l_{abl}^{n-eq} < l_{abl} < l_{abl}^{max}$. The maximum ablation depth is defined by the condition that the kinetic energy of ablated atoms is zero:

$$l_{abl}^{max} = \frac{F_a}{n_a (\varepsilon_b + J)} \quad (3)$$

The ablation depth is a minimum for given fluence (non-thermal depth) when kinetic energy of ablated atoms is a maximum, $l_{abl}^{n-eq} = 0.5 l_{abs} \ln(F_a / F_{thr})$. Then the total number of atoms ablated per pulse is $N_{abl} = n_a V_0 \equiv n_a S_{foc} l_{abl}$ (S_{foc} is the focal spot area). The total number of carbons in the plume, N_{abl} , and their initial temperature, T_0 , define the initial conditions for the plume expansion accompanied by the cluster formation. For the experimental conditions of this work ($F_a = 2 \text{ J/cm}^2$; $S_{foc} \sim 10^{-5} \text{ cm}^2$; $F_a / F_{thr} = 10$) one obtains $l_{abl}^{n-eq} \approx 3.45 \cdot 10^{-6} \text{ cm} < l_{abl} < l_{abl}^{max} = 5.6 \cdot 10^{-6} \text{ cm}$; the average value is $l_{abl} \sim 4.5 \times 10^{-6} \text{ cm}$; $l_{abs} \sim 30 \text{ nm}$; $A \sim 0.55$; $V_0 = 4.5 \times 10^{-11} \text{ cm}^3$; $T_0 = 24.2 \text{ eV}$; $\varepsilon_b + J \sim 15 \text{ eV}$); where the initial velocity of carbon is $v_1 = (2T_0 / m_c)^{1/2} = 2 \times 10^6 \text{ cm/s}$; $N_{abl} = 5.1 \times 10^{12}$.

4.2. Kinetics of cluster formation

On the basis of the previous studies of carbon nanotubes and carbon nanofoam formation [1,4] one can suggest that the carbon clusters are created at a temperature higher than or close to $T_{min} \sim 1200 \text{ K}$. Let's take this temperature as a limit temperature for cluster formation in a plume: that is clusters cannot be formed if the temperature drops below this value. The expanding plume of ablated carbons cools down adiabatically either due to diffusion in the ambient gas or by expansion in vacuum. We define the time appropriate for cluster formation as a time when temperature in the plume is greater than the above limit. It follows [1,4] that carbon-to-carbon and carbon-to-cluster sticky collisions (monomer addition) play a major role in cluster formation. Moreover, the carbon-to-carbon collision time is an appropriate scaling time for estimation of the maximum number of carbons, which can stick together. We estimate the maximum number of carbons that could be attached together as a ratio of the time when temperature is above the appropriate minimum, to the time of carbon-carbon collision.

4.3. Carbon cluster formation in ambient gas

Shock wave. Immediately after the pulse end the shock wave starts to propagate into the gas. The shock front is smeared over a distance comparable to the carbon mean-free-path in a gas $l_{mfp} = (n_{Ar} \sigma)^{-1}$. For 50 Torr Argon ($n_{Ar} = 3 \times 10^{18} \text{ cm}^{-3}$) this equals $l_{mfp} = 3.33 \times 10^{-4} \text{ cm}$. The shock wave ceases to exist at $r = (3E_p / 4\pi P_{Ar})^{1/3} \sim 2.2 \times 10^{-2} \text{ cm}$ ($E_p = 2 \times 10^{-5} \text{ J}$), when the pressure behind the shock becomes comparable with the gas pressure. However, at this stage the plume-argon mixture is completely cool and thus we ignore the shock stage in the future estimates.

Diffusion. Diffusion of single carbons in ambient gas of density n_{ar} proceeds with diffusion velocity, $D_1 = l v_{carb} / 3 \approx v_{carb} / (3n_{Ar} \sigma)$. Here σ is the cross section for carbon-carbon elastic collisions which is taken the same as that for hard sphere collisions. For example, taking $\sigma \sim 10^{-15} \text{ cm}^2$; $n_{ar} \sim 3 \times 10^{18} \text{ cm}^{-3}$ (which corresponds to $\sim 50 \text{ Torr}$ of Argon) one obtains $D \sim 2.5 \times 10^2 \text{ cm}^2/\text{s}$. We will assume that the average temperature of the carbon-argon mixture, T_{min} , is achieved at the instant t_{min} , when the

diffusion front reaches a distance R_l , and the volume occupied by plume equals to V_l where $R_l \approx (D_l t_{\min})^{1/2}$.

Carbon cooling proceeds in two overlapping stages. Adiabatic expansion into volume V_l occurs accompanied by temperature equilibration between carbon and argon. The temperature after the adiabatic expansion with adiabatic constant γ reads:

$$T_{ad} = T_0 (V_0 / V_l)^{\gamma-1} \quad (4)$$

Then the volume V_l is obtained from the condition that temperature after equilibration equals the above-defined minimum temperature:

$$T_{\min} = T_{ad} \cdot \frac{n_c}{n_{ar} + n_c} = \frac{T_0 \cdot n_c}{n_{ar} + n_c} \left(\frac{V_0}{V_l} \right)^{\gamma-1} \quad (5)$$

Here n_c is the partial number density of carbons in volume V_l where $n_c = N_{abl} / V_l = n_0 V_0 / V_l$. Then, V_l (or t_{\min}) can be obtained from the solution of the following algebraic equation:

$$\frac{T_{\min}}{T_0} = \frac{x^{-(\gamma-1)}}{1 + n_{ar} \cdot x / n_0}; \quad x = \frac{V_l}{V_0} \gg 1 \quad (6)$$

For all pressures of Argon we have $n_{ar} / n_0 \ll 1$. Thus, a good first approximation is:

$$x = V_l / V_0 \approx (T_0 / T_{\min})^{1/(\gamma-1)} \quad (7)$$

Taking $T_0 = 24.2$ eV; $T_{\min} \sim 0.1$ eV, and $\gamma = 5/3$ one obtains $V_l = V_0 (224)^{3/2} = 3.35 \times 10^3 \times V_0$ proving the approximation is good for description of our experiments. We assume that one-dimensional expansion takes place ($S_{foc}^{1/2} > R_l$), therefore $V_l = S_{foc} R_l$. The expression for cluster formation time is as follows:

$$t_{\min} = \frac{3n_{ar}\sigma}{v_{carb}} \cdot \left(\frac{V_0}{S_{foc}} \right)^2 \cdot \left(\frac{T_0}{T_{\min}} \right)^{2/(\gamma-1)} \quad (8)$$

Taking $\sigma \sim 10^{-15}$ cm²; $n_{ar} \sim 3 \times 10^{18}$ cm⁻³; one obtains $t_{\min} \sim 10^{-6}$ s.

Maximum cluster size. The time for a carbon-carbon collision at density n_c in volume V_l reads:

$$t_{sticky} = (n_c \sigma_{att} v_c)^{-1} = \frac{V_l}{V_0} \frac{1}{n_0 \sigma_{att} v_c} = \frac{1}{n_0 \sigma_{att} v_c} \left(\frac{T_0}{T_{\min}} \right)^{1/(\gamma-1)} \quad (9)$$

Note that the attachment cross section is unknown, and it is definitely lower than elastic cross section taken for diffusion above. The maximum number of carbons that can be combined together to form a cluster is estimated as follows (taking $\gamma = 5/3$):

$$N_{\max} \approx \frac{t_{\min}}{t_{sticky}} = 3n_0 \cdot n_{ar} \cdot \sigma \cdot \sigma_{att} l_{abl}^2 (T_0 / T_{\min})^{3/2} \quad (10)$$

For our experimental conditions one gets $N_{\max} < 7 \times 10^4$. This corresponds to the cluster radius:

$$r_{cluster} = (N_{\max} / (4\pi n_0 / 3))^{1/3} \sim 5.3 \text{ nm.}$$

4.4. Cluster formation by single pulse in vacuum

Carbon clusters can be formed in an adiabatically expanding plume in vacuum until the temperature drops to the minimum temperature for cluster formation, T_{\min} . The plume volume at that instance in accordance to (4) reads:

$$V_l = V_0 \cdot (T_0 / T_{\min})^{1/(\gamma-1)} \quad (11)$$

In the one-dimensional expansion case one easily obtains the plume volume as $V_l = S_{foc} t_{\min} v_{carbon}$, and maximum time allowed for the cluster formation as $t_{\min} = V_l / (S_{foc} v_{carbon})$.

Taking $t_{sticky} = V_l / (V_0 n_0 \sigma_{att} v_c)$ the maximum number of atoms per cluster with the sticky collision time taken in accordance to (11) is as follows:

$$N_{\max} \approx t_{\min} / t_{\text{sticky}} = n_0 \cdot \sigma_{\text{att}} \cdot l_{\text{abl}} \quad (12)$$

In the experimental conditions of this paper the above formulae gives $N_{\max} \sim 500$ atoms and $r_{\text{cluster}} \sim 1$ nm, which is in qualitative agreement with the experimental data. We note that the average carbon density in the formation zone comprises $n_c \sim 3.37 \times 10^{19} \text{ cm}^{-3}$, which is comparable to the number density at atmospheric pressure. This is the reason why the carbon cluster form during only a single pulse and in vacuum. However, this density is an underestimate for the carbon density for cluster formation because the spatial density distribution in adiabatic expansion is steep and the contribution of higher density areas into formation process should be significant. We will consider this problem elsewhere.

5. Discussion and conclusions

The salient feature of our findings that has not been uncovered to date to the best of our knowledge is an almost complete independence of the cluster size on the conditions in the chamber. Change of the gas (from helium to xenon) and change of the gas pressure in a range from 20 mTorr to 200 Torr does not affect the average cluster diameter that was found to be 4 ± 0.5 nm. The above analysis suggests that the average density of carbons in the cluster forming zone in vacuum and with gas pressures used in experiments was approximately $3.5 \times 10^{19} \text{ atoms/cm}^3$, which is comparable to that of atmospheric pressure. Therefore in all our experiments, the dependence on the parameters of background gas is weak because $n_{\text{carbon}} \gg n_{\text{gas}}$.

It is also instructive to compare the experimental results for silicon cluster formed in vacuum using a femtosecond laser which were reported recently [2]. Silicon nanoclusters of average size 8 ± 2 nm were formed by laser ablation (800 nm; 120 fs; 1kHz-3Hz. $F = 5 \text{ J/cm}^2$) in vacuum. An estimate for the average size of silicon cluster in these conditions by formula (14) and taking ablation depth of 7.7×10^{-5} cm gives the cluster radius of 2.7 nm. The simple model used above underestimates the cluster size in vacuum for both carbon and silicon clusters [2] because it ignores the steep spatial density distribution during the adiabatic expansion. We will present the model with this effect taken into account elsewhere. However, the replacement of constant density by a two-step distribution already results in doubling of the average cluster size. The presence of a buffer gas with pressure range 20 mTorr to 200 Torr weakly affects the single-cluster formation process, however, at higher pressures; it serves to prevent the formation of a film containing clusters, instead producing the foam-like structure.

To conclude we found that a single laser pulse can form carbon nanoclusters in vacuum, with well-defined size. The cluster size should, in a broader parameter range than that used in the above experiments, depend more visibly on the combination of laser and target parameters. Our experiments and analysis suggest that the pressure of the ambient gas may affect the cluster size if the gas density is greater than carbon density in the formation zone. This means the ambient gas should be 1-2 atmospheres or higher to observe a dependence of cluster size. It is also worth mention that there is a possible interaction between the proceeding laser pulses and the already-formed nanoclusters in the plume, which may affect cluster size. We will investigate this possible interaction in the future.

Acknowledgements

The support of the Australian Research Council through its Centre of Excellence and Federation Fellowship programs is gratefully acknowledged.

References

- [1] E. G. Gamaly, A. V. Rode, *Nanostructures created by lasers*, in: *Encyclopaedia of Nanoscience and Nanotechnology*, Ed. H. S. Nalwa, American Scientific Publishers, Stevenson Range, 2004, v. 7, 783-809.
- [2] S. Amoroso, R. Bruzzese, N. Spinelli, et al., *Appl. Phys. Lett.* **84**, 4502 (2004).
- [3] B. Luther-Davies, V. Z. Kolev, M. J. Lederer, et al., *Appl. Phys. A* **79**, 1051 (2004).
- [4] A. V. Rode, E. G. Gamaly, and B. Luther-Davies, *Appl. Phys. A* **70**, 135 (2000).
- [5] E. G. Gamaly, A. V. Rode, B. Luther-Davies, and V. T. Tikhonchuk, *Physics of Plasmas*, **9**, 949-957 (2002).